Resolving power in liquid chromatography: A trade-off between efficiency and analysis time

Dores-Sousa, Jose Luis; De Vos, Jelle; Eeltink, Sebastiaan

Published in:
Journal of Separation Science

DOI:
10.1002/jssc.201800891

Publication date:
2019

Document Version:
Accepted author manuscript

Resolving power in liquid chromatography: A trade-off between efficiency and analysis time

José Luís Dores-Sousa, Jelle De Vos, and Sebastiaan Eeltink*

Vrije Universiteit Brussel (VUB), Department of Chemical Engineering, Brussels, Belgium

(*) corresponding author

Pleinlaan 2, B-1050, Brussels, Belgium

Tel.: +32 (0)2 629 3324, Fax: +32 (0)2 629 3248, E-mail: sebastiaan.eeltink@vub.be

Abstract

This review describes chromatographic dispersion and different plate-height models frequently used to assess the chromatographic performance of (UHP)LC column technology. Furthermore, different performance indices, including the resolution, the separation impedance, and kinetic plots are discussed allowing to quantify and visualize the resolving power in liquid chromatography. The construction of kinetic plots is explained, and different visualization approaches are highlighted. Finally, key instrument and column-technology developments to advance the kinetic performance limits are discussed and selected state-of-the-art applications are highlighted.

Keywords: UHPLC, ultra-high-pressure liquid chromatography, van Deemter curve, kinetic performance, kinetic plot

1. HPLC: historical overview

The discovery of chromatography dates back to 1903, when Mikhail Tswett's research in the botanic field led to the development of an adsorption technique capable of separating leaf pigments [1]. He proved the existence of different binding molecular forces by separating chlorophyll in its different constituents, by conducting a separation experiment utilizing a narrow tube packed with different adsorbents and eluting fractions using mobile phases with different solvent strength yielding different colored fractions. This adsorption phenomena became known as "chromatography" years later, which comes from the Greek *chroma* (color). Other major milestones in the development of separation science are the development of ion-exchange chromatography as part of the Manhattan Project in World War II to separate and identify products from uranium fission and the achievements of Nobel Prize in Chemistry laureates Archer Martin and Richard Synge [2,3]. They aimed to develop an apparatus to perform liquid-liquid countercurrent extraction, equivalent to two hundred separatory funnels, in an attempt to separate acetylamino acids. While the initial experiment failed, they successfully immobilized one of the liquid phases (water) on a solid support and moved the other immiscible liquid (chloroform) through a packed tube and hence developed liquid-liquid partition chromatography [4]. In a later experiment, the liquid mobile phase was replaced by a gas vapor, which gave rise to the emergence of gas chromatography [5].

The first report on modern HPLC, *i.e.*, the ion-exchange separation of nucleotides and cellular extracts, was published in 1967 by C. Horváth [6]. In the early 1970's the first commercial instrument was introduced [7] and shortly after, in 1973, columns packed with 10 μm silica C_{18} particles became commercially available [8]. To advance separation performance aiming at higher efficiencies, there has been an on-going trend towards using columns packed with small particle diameters [7,9]. At the same time significant progress has been realized with respect to functionalization of the surface chemistry of the particles, greatly increasing chromatographic reproducibility [10]. A landmark paper published in 1997 by MacNair and Jorgenson on the use of ultra-high pressures in LC in combination

with capillary columns packed with 1.5-micron particles ultimately led to a revolution in the field of separation science [11]. In 2004, the first ultra-high-pressure LC instrument capable of working at 1000 bar operating pressure was introduced together with 2.1 mm I.D. columns packed with 1.7 μm particles [12]. Currently, UHPLC technology is broadly established and instruments allowing to operate up to 1500 bar are commercially available. Furthermore, significant advances in stationary-phase design have been realized with respect to mechanical stability, particle size and homogeneity, and particle type, significantly yielding better chromatographic performance limits [13,14].

2. Resolution

Giddings defined the resolution (R_s) as "*the most important index of success for the analytical separation of two specific components*" [15]. In mathematical terms, R_s is a measure of the degree of separation of zones defined by the difference in retention times (Δt_R) between the two zones with respect to zone dispersion characterized by the baseline peak width (4σ), defined as [16]:

$$R_s = \frac{\Delta t_R}{4\sigma} = \frac{\sqrt{N}}{4} \cdot \left[\frac{k_2}{1+k_2}\right] \cdot \left(\frac{\alpha - 1}{\alpha}\right) \quad (1)$$

assuming that two adjacent peaks have identical peak widths [17]. Whereas the distance between two peaks centers, Δt_R, increases linearly with the distance traveled in the column, σ increases proportional to the square root of L, see Fig. 1A [15]. With increasing selectivity, the incremental distance (Δt_R) increases more rapidly with L, crossing the 4σ line sooner and thus unit resolution is achieved in a shorter migration distance. With a $R_s = 1$ the percentage of separation between the peaks is 95.4% [18]. Baseline resolution between the peak pair is achieved when $R_s \geq 1.5$.

Using the classical resolution equation as a starting point, Purnell derived the resolution as function of plate number (N), retention factor (k), and selectivity factor (α), see the right-hand side of Eq. 1. Fig. 1B shows the effect of N, k, and α on the resulting change in R_s. The most rewarding

parameter affecting R_s is the selectivity. Typical values for α range between 1 and 2, and this corresponds to a variation from 0.001 up to 1 in the term $(\alpha - 1)/\alpha$. The k of the critical pair is generally tuned to reach a value between 3 and 5 (for separations conducted in isocratic mode), which consequently leads to the shortest possible analysis time [19]. This can either be achieved by optimization of the stationary-phase chemistry, tuning the mobile-phase composition with respect to elution strength, or a combination of both. Finally, the separation can be fine-tuned by optimizing N via a change in stationary-phase support, *i.e.*, particle size of packed columns, and/or column length. Optimization of resolution via N follows a square root dependency and is therefore less rewarding. Since the resolution differs for each specific peak pair, it cannot be used as a generic metric to describe the quality of a separation. α and k are largely controlled by the types of analytes in the sample and hence the separation/mobile-phase system selected. Hence, to achieve the desired separation performance within the shortest possible time frame, a good understanding of separation efficiency as function of analysis time is vital.

3. Chromatographic dispersion and plate-height equations

The separation of an analyte mixture in its individual components can be achieved by differential migration, where the molecules follow a random path in the column and equilibria are established between the mobile and stationary phase. As such, each analyte band inside the column can be assumed to follow a statistical distribution of molecules and the width is proportional to its variance (σ_L^2). The variance increases proportionally with the distance traveled in the column (L). The slope of this relation is defined as the plate height (H), which allows to compare chromatographic dispersion independent of the position of the peak in the column. Since the retention time (t_R) is proportional to L, the plate height (H) can also be expressed as function of time units, according to [20]:

$$H = \frac{{\sigma_L}^2}{L} = \frac{L \cdot {\sigma_t}^2}{{t_R}^2} \quad (2)$$

H is a column length-independent parameter to assess the efficiency. If divided by the column length *L* the number of plates (*N*) can be determined which is proportional to the retention time and peak width ratio, according to Eq 3:

$$\frac{H}{L} = \frac{{\sigma_t}^2}{{t_R}^2} = \frac{1}{N} \Leftrightarrow N = \frac{L}{H} \quad (3)$$

Based on the pioneering work of Martin and Synge, different plate-height models have been derived, describing *H* as function of the linear flow velocity (u_0). The van Deemter equation describes the plate height as the sum of three independent contributions, see Eq. 4, σ increases proportional to the square root of *L*, see Fig. 1A and their addition provides a curvilinear relationship as function of u_0, as depicted in Fig. 2 [21].

$$H = A + \frac{B}{u_0} + C \cdot u_0 \quad (4)$$

The eddy dispersion or *A*-term contribution, schematically depicted in Fig. 3A, is flow-rate independent and its magnitude is affected by differences in flow velocities experienced in a multitude of flow paths. H_A is proportional to the characteristic size, *e.g.*, particle size (d_p) for packed columns, and the heterogeneity of interstitial space. The second contribution, longitudinal diffusion or the *B*-term (Fig. 3B), describes chromatographic dispersion induced by Brownian motion. H_B is inversely proportional to u_0 and is proportional to the analyte diffusion in the mobile (D_m) and stationary phases (D_s). The *C*-term describes the resistance to mass transfer between the stationary and mobile phase, *i.e.*, the molecules are transported in the mobile phase and reversibly adsorb/desorb to the stationary-phase surface, see Fig. 3C [22]. Differences in velocities between molecules and the kinetics of the absorption-desorption process involve the mass-transfer process from the mobile phase to the surface of the stationary phase (C_m-term) and *vice versa*, and diffusion of analytes inside the pores within the stationary phase filled with stagnant mobile phase (C_s-term). At low linear velocity, *H* is dominated

by longitudinal diffusion, whereas at higher linear velocities the mass-transfer processes become dominant. The optimal mobile-phase velocity (u_{opt}) increases when the particles size (d_p) is decreased and the corresponding minimum plate height (H_{min}) is proportional to particle size, according to:

$$u_{opt} = \sqrt{\frac{B'}{C'}} \cdot \frac{D_m}{d_p} \tag{5}$$

$$H_{min} = \left(A' + 2\sqrt{B' \cdot C'}\right) d_p \tag{6}$$

An alternative plate-height equation was introduced by Giddings, who postulated that mobile phase dispersion, *i.e.*, the tortuous flow contribution (*A*-term) and mass transport in the mobile phase (C_m-term) affect dispersion in parallel and hence are interlinked [20]:

$$H = \frac{B}{u_0} + C_s \cdot u_0 + \left(\frac{1}{A} + \frac{1}{C_m \cdot u_0}\right)^{-1} \tag{7}$$

In a more detailed view, coupling the bed dispersion and the mobile-phase mass transfer, Giddings defined five categories of velocity differences in a column, *i.e.*, transchannel, transparticle, short-range interchannel, long-range interchannel, and transcolumn velocities, see Fig. 4, that can be used to extend the plate-height equation to:

$$H = \frac{B}{u_0} + C_s \cdot u_0 + \sum_{1}^{5} \left(\frac{1}{A} + \frac{1}{C_m \cdot u_0}\right)^{-1} \tag{8}$$

This results in a more accurate theoretical model but a rather complex plate-height equation, for which experimental verification has not been delivered. Alternatively, Knox *et al.* derived an empirical plate-height equation that describes the flow dependent behavior of the *A*-term, with an exponent of the velocity that commonly has an assigned value of 1/3 based on fitting a large number of chromatographic data [23]:

$$h = a \cdot v^{1/3} + \frac{b}{v} + c \cdot v \tag{9}$$

Comparing the performance of different separation media is not straightforward. Giddings proposed dimensionless parameters as universal units to compare the packing quality of columns

independently of column length, column diameter, and particle size [20]. The reduced plate height (h) and reduced velocity (ν) are defined as:

$$h = \frac{H}{d_p} \tag{10}$$

A value of $h_{min} < 2.4$ indicates a "well" packed column and good system performance with respect to extra-column dispersion [23]. The reduced velocity (ν) is given by:

$$v = \frac{u_0 \cdot d_p}{D_m} \tag{11}$$

4. Kinetic performance limits

Kinetic performance is a quality index for the chromatographic performance that provides information about the separation efficiency per unit time, while incorporating the effect of column pressure on the separation. The concept of such a '*performance index*' (π) was first introduced by Golay when comparing the efficiencies of different column types, *i.e.*, open-tubular and packed columns, in GC mode [24]:

$$\pi = \frac{N}{t_R} \cdot \frac{N}{\Delta P} = \frac{N^2}{t_R \cdot \Delta P} \tag{12}$$

It represents the number of plates generated per unit time multiplied by the number of plates generated per unit pressure drop. To account for differences in mobile-phase viscosity and make the performance index more generic with respect to the effect of mobile-phase composition on retention factor, Bristow and Knox introduced the '*separation impedance*' (E), defined as [24]:

$$E = \frac{t_R \cdot \Delta P}{N^2 \cdot \eta \cdot (1 + k_2)} = \frac{H^2}{K_v} = h^2 \cdot \phi \tag{13}$$

where ΔP is the pressure drop across the column, and η the mobile-phase viscosity. The lower the value of E the better is the column performance. Optimizing the kinetic performance of the chromatographic system involves minimizing the plate-height value by operating the column at

conditions, which correspond to the minimum of the van Deemter curve. Columns with a high column permeability (low flow resistance) intrinsically yield better performance limits, provided that high separation efficiency is maintained. A Typical *E* value for columns packed with fully porous particles is 3000 (with h_{min} ~ 2 and ϕ of 750) and *E* reaches as low as 20 for coated capillaries (*h* at optimal conditions of 0.8 and a flow resistance of 32).

Only a few years after the introduction of the concept of π, Giddings proposed a graph in 1965 visualizing the separation time in gas and liquid chromatography as a function of the number of required plates while operating columns at the maximum inlet pressure [25]. The concept of '*kinetic plots*', *i.e.*, visualizing the kinetic performance limits of a chromatographic system has been refined to provide information on what separation system and/or which column-length/particle-size-combination should be utilized to yield the desired separation efficiency within the shortest possible analysis time. For the construction of the graph representing kinetic performance limits in terms of efficiency and analysis time in isocratic mode, experimental plate-heights and pressure data can be transformed and extrapolated to yield the performance when operating the column at the maximum operating/system pressure (ΔP_{max}), by [26,27]:

$$N = \frac{\Delta P_{max}}{\eta} \cdot \left(\frac{K_v}{u_0 \cdot H}\right)_{exp} \tag{14}$$

$$t_0 = \frac{\Delta P_{max}}{\eta} \cdot \left(\frac{K_v}{{u_0}^2}\right)_{exp} \tag{15}$$

Fig. 5. depicts the principle to construct a kinetic plot from experimental plate-height data. The analysis time (in terms of t_0) is provided as function of *N* obtained on a 50 mm column packed with 3 μm particles when operating at different flow rates. Hence, the *B*-term region is situated at high t_0 times, and the *C*-term region at low t_0 values. In u_{opt} this column is operated at 40 bar (excluding system contribution to operating pressure). At a maximum system pressure of, for example, ΔP_{max} of 400 bar, the column length can be increased by a factor 10, hence increasing both t_0 and *N* proportional to column length (taking into account the column permeability). When operating the column at a

higher flow rate, *e.g.*, yielding a column pressure of 200 bar, the column length can be doubled before the maximum operating pressure is reached. By connecting the resulting (extrapolated) data points the '*kinetic performance limit curve'* is obtained that represent the best possible performance for a specific system, *i.e.*, in this case the highest *N* with the shortest possible time for columns packed with 3 μm particles and a maximum operating pressure of 400 bar. Short columns yield short t_0 times with relatively low plate numbers and t_0 and *N* increases as function of column length. The performance-limit curve approaches a vertical asymptote reflecting the *B*-term dominated region where the maximum plate number is obtained. It should be noted that by performing the extrapolation using Eqs. 14 and 15 it is assumed that columns are equally well packed and hence exhibit similar *E*-values and that the effect of extra-column dispersion induced by column coupling can be neglected. A detailed description of kinetic plots and its experimental validation has been described by Cabooter *et al*. [28,29], and de Villiers *et al*. [30], among others. Note that for very short columns packed with small diameter particles yield very low peak volumes (< 0.5 μL) for early-eluting analytes on 50 mm long columns packed with 1.5 μm particles [31] extra-column contribution induced by injection, connection tubing and/or the volume of the detector flow cell will ultimately become significant. Furthermore, when raising the pressure limit of the system above 400 bar, radial and axial temperature gradients due to viscous heating will affect the retention properties and/or the efficiency observed. The magnitude strongly depends on the column diameter and also the oven configuration, *i.e.*, a still-air or forced-air oven, utilized [32].

Kinetic plots have been used as a geometry-independent method to compare the kinetic performance of different LC supports [26] and to visualize the enhancement of performance limits when increasing the pressure rating of instruments. The kinetic plot depicted in Fig. 6. shows the effect of particle size (1.7, 3, and 5 μm) and operating pressure (400 *versus* 1500 bar operation) on the resulting performance. Different regions can be distinguished where one column-length/particle-size combination outperforms another. Short columns packed with small particle diameters provides

the best kinetic performance when sample throughput is pursued, and for high-efficiency separations columns packed with larger particles provides the better compromise in efficiency per unit time. The intersection where the Knox-and-Saleem limit curve touches the kinetic plot represents the optimal mobile-phase velocity (when E_{min} is reached) for each separation system, *i.e.*, the point where the best kinetic performance is achieved for a specific column-length/particle-size combination. In this case, the minimum analysis time to achieve the maximum number of plates is defined as [33]:

$$t_{0,min} = \left[\frac{H^2{}_{min}}{K_{v,0}} \cdot \frac{\eta}{\Delta P_{max}}\right] \cdot N^2 = \left[E_{min} \cdot \frac{\eta}{\Delta P_{max}}\right] \cdot N^2 \tag{16}$$

To quantify the gain in either separation efficiency or analysis time when moving from a conventional LC approach towards a fully-optimized system performance at maximum system pressure, Desmet *et al.* derived the time (G_t) and efficiency gain factor (G_N) defined as [34]:

$$G_t = \frac{t_{0,exp}}{t_{0,min}} = \frac{E_{exp}}{E_{min}} \cdot \frac{\Delta P_{max}}{\Delta P_{exp}} \tag{17}$$

$$G_N = \frac{N_{max}}{N_{exp}} = \sqrt{\frac{E_{exp}}{E_{min}} \cdot \frac{\Delta P_{max}}{\Delta P_{exp}}} \tag{18}$$

Note that maximum gain factor is reached when operating the system at ΔP_{max} while the column is operated at the optimum flow velocity (E_{min}). Fig. 6 also shows that increasing the maximum operating pressure in LC affects the position of the Knox-and-Saleem limit (see the gray area representing the performance allowed when the maximum pressure is limited to 400 bar *versus* the Knox-and-Saleem limit for 1500 bar, represented by the red dotted line) and that the separation efficiency per unit time increases. Eq. 17 shows that the decrease in analysis time is proportional to the increase in maximum pressure, whereas Eq. 18 shows that the gain in efficiency comprises only a square root dependency. Kinetic gain factors using state-of-the-art UHPLC technology were experimentally validated by De Vos *et al.* [31]. Recently, Blumberg and Desmet introduced a column kinetic performance factor as measurable dimensionless metric of trade-off between separation efficiency, time, and pressure [35].

To aid the interpretation of the chromatographic performance limits, different visualization approaches have been proposed in addition to the t_0 *versus* N representation used in Fig. 6. Hans Poppe proposed a graph plotting plate time (t_0/N) *versus* plate number (N) to obtain a more expanded view on the kinetic performance in the *C*-term region (where the kinetic plot approaches a horizontal asymptote), see Fig. 7A [26]. Desmet *et al.* showed the advantages of different representation approaches, including plotting t_0/N^2 as function of N to magnify differences in *C*-term effects [26]. In order to allow for an interpretation of *B*-term and *C*-term regions in a similar fashion of the classical van Deemter curve the x-axis has been inverted, see Fig. 7B. The minima in the kinetic plots represent the respective Knox-Saleem limits for different support structures. Eeltink *et al.* plotted the effective plate number (N_{eff}), defined as:

$$N_{eff} = N \cdot \frac{k^2}{(1+k)^2} \tag{19}$$

as a function of analysis time to ensure that the data points relate to the same chromatographic resolution which allows for an unbiased comparison of the kinetic performance of columns with different phase ratios [36].

In gradient mode the peak capacity (n_c) has been most frequently used as performance indicator, defined by [37,38]:

$$n_c \approx \frac{1}{R_s} \cdot \frac{t_G}{4\sigma} = \frac{1}{R_s} \cdot \frac{t_G}{t_0} \cdot \frac{\sqrt{L}}{4(1+k_{elut})\sqrt{H_{grad}}} \tag{20}$$

where the ratio of the gradient time (t_G) with respect to t_0 time is related to the gradient steepness and the magnitude of the plate height in gradient mode (H_{grad}) is dependent on retention factor experienced by the analytes when eluting from the column (k_{elut}). Mathematical expressions to extrapolate the gradient performance measured at different flow rates resulting into kinetic plots have been discussed by Broeckhoven *et al.* [39]. The data transformation is based on the assumption that H and η are independent of column length. Hence, when operating at different flow rates, the gradient time needs

to be adjusted such that the t_G/t_0 ratio is maintained constant. Furthermore, the ratio of the dwell time with respect to t_0 time needs to be kept constant, but this constraint is often omitted for reasons of practicality. The principles and practice to create gradient kinetic plots have been reviewed by Causon *et al.* [40].

5. Advancing performance limits and selected examples

Over the last two decades major technology developments with respect to instrumentation and column technology have led to significant breakthroughs in the resolving power realized. Here, we highlight the key technology and corresponding application development in the field of one-dimensional RP-LC separations focusing on kinetic performance limits.

Currently, most vendors offer UHPLC instrumentation with maximum pressure capabilities between 1300 and 1500 bar that are compatible with 2.1 mm I.D. column formats packed with sub-2-micron particles. Significant advances in instrumentation design has been pursued to maintain the high separation efficiency offered by the current state-of-the-art HPLC columns while realizing accurate flow delivery and robust performance. Many of these tubings are handled tool-free and are available in a biocompatible metal alloy. Especially when operating sub-2-µm columns at high flow rates it is mandatory to select short connection tubing with a small I.D. to avoid excessively large pressure drops over the tubing and loss in efficiency. Future designs of UHPLC equipment will possibly strive to minimize the number of connections and tubing, *i.e.*, by integrating fluidic pathways, similar to what can be obtained in advanced microfluidic platforms. Major developments include new pump designs that account for solvent compression and heating effects when operating at ultra-high pressure [32]. Applying unique feedback systems, the piston speed can be adjusted as function of gradient composition and pressure to ensure constant flow-rate delivery [41]. Furthermore, to minimize the pressure ripple during injection different approaches towards sample precompression, prior to in-line switching of the sample loop with the column, have been designed

[42]. A mandatory innovation was to employ materials that meet the operating standards of modern UHPLC equipment. Different materials, each one having their own characteristics and function, are used to build the different modules of the UHPLC system. These include metallic alloys, synthetic crystalline solids, polymers, and composite materials. The wetted parts of the system also have the extra demand that they need to be inert to the sample (*e.g.*, sample needles and injection valves) but also to the employed mobile phase (*e.g.*, pump heads and seals). Some manufacturers even offer a modified UHPLC system configuration that is compatible with biological samples. To improve biocompatibility, many parts modules are adapted to minimize the release of dissolved metal ions in the fluidic pathway [32]. A main characteristic for materials employed in the high-pressure flow path of the LC equipment, is that they need to possess a high mechanical stability to withstand material stresses due to the applied high pressures and/or temperatures and related frictional forces due to the liquid flow. Typically used materials in the pump head are stainless steel and titanium alloys, to ensure the robustness of the high-pressure duty cycles. Often ignored, the material choice of the injection valve is equally important. High-pressure fluidic injection pulses combined with the rotary shear forces impose large forces on the rotor and stator. To improve wear resistance, the latter is often coated with diamond-like carbon or composite materials, whereas rotors are made from proprietary polymer or composite materials.

To mitigate axial and radial temperature gradients in the column induced by frictional heating the effect of column thermostatting using either forced- or still-air oven configurations have been explored extensively [32,43,44]. When operating a 10 cm column packed with 1.5 µm core-shell particles at the optimal flow rate, baseline peak widths of 0.34-3 s are expected for retention factors between 0 and 8. Therefore, a new type of optical waveguide was introduced for UV/Vis spectrophotometric detectors based on total reflection. This allowed to design sub-µL sized flow cells which, combined with higher acquisition rates, is mandatory to reliably detect peaks from a state-of-the-art UHPLC column. A detailed description of advances in instrument design has been described

in a review by De Vos *et al.* in 2016 [32]. The Jorgenson group is one of the frontier groups in designing UHPLC instrumentation allowing to operate columns up to a maximum pressure of 7100 bar. Fig. 8. shows the isocratic RP-LC separation of small-molecular-weight analytes operating a 45-cm long capillary column packed with 1 μm non-porous particles at 7100 bar in only 240 s, yielding plate numbers ranging between 310,000 and 196,000 [45].

To advance the chromatographic performance limits further, significant progresses in column technology has been realized. On the one hand, new approaches to reducing *H* have been pursued. On the other hand, improving performance limits have been realized using column technology characterized by higher column permeabilities (see Eqs. 14 and 15). Considering packed column technology, the current state-of-the-art commercially-available columns for high-throughput separations are currently packed with 1.3 μm core-shell particles [46]. It should be noted however that column packing of microparticulate columns is still highly challenging. Reising *et al.* reconfirmed the importance of eddy dispersion on separation efficiency induced by packing heterogeneity [47,48]. Chromatographic and morphological characterizations of slurry-packed columns (at constant pressure) revealed that the most homogeneous bed microstructure and hence highest separation efficiency is obtained towards the column outlet [47]. In a study conducted by Billen *et al*., it was demonstrated that also the particle-size distribution and especially the presence of fines significantly affects the *A*-term contribution to chromatographic dispersion [49]. Bruns *et al.* demonstrated the improved trans-column packing homogeneity induced when packing columns with (core-shell) particles characterized by a narrow particle-size distribution. This group observed that core-shell particles pack denser and with a higher regularity near the column wall (closer to the bulk packing density) compared to fully-porous particles having a broader particle-size distribution [50]. A significant advancement in kinetic performance has been achieved by the introduction of (sub-3-micron) core-shell particle technology [51,52]. An overall reduction of approximately 25% in H_{min} has been measured, induced by the lower *A*-, *B*-, C_m-, and C_s-contributions to chromatographic

dispersion [31]. Furthermore, a 20-30% increase in column permeability results in better performance limits due to the more proficient column-length/particle-size-combination [53]. In a recent study conducted by Wei *et al.* the synthesis and application of core-shell particles containing elongated pore channels has been demonstrated, yielding reduced plate height (h_{min}) as low as 1 [54]. In a computational-fluid-dynamics study conducted by Deridder *et al*. it was demonstrated that this efficiency increase could be attributed to the reduced *B*-term contribution, while the *C*-term remained unaffected [55].

The most common alternative column format to microparticulate-packed columns are the monolithic columns formats and coated capillary columns. A monolithic column is composed of an interconnected network of polymer microglobules or silica skeletons percolated by macropores [56-58]. Originally, monolithic materials were tuned towards high permeability, allowing the use of long column formats for high plate-number separations. To outperform conventional packed columns, much effort has been directed to tune both the feature sizes (globule/skeleton size and the diameter of the macropores) while maximizing the porosity [59,60]. Motokawa *et al.* has described the preparation and evaluation of silica monolithic columns with different skeleton sizes and macropore sizes by optimizing the precursor to porogen ratio [61]. The potential of silica monolithic columns has been demonstrated for both small molecular-weight analytes [61-65] and gradient separations of peptides [62,66-68] and proteins [66,69]. A similar approach has been followed for the preparation of polymer monoliths [70,71]. For example, Vaast *et al.* developed high-porosity polymer monolith entities exceeding 70% while decreasing the characteristic size (I.D. of macropores and globule size) to reduce the plate height. Utilizing nanostructured porous polymer monolithic columns at UHPLC conditions (800 bar) both highly efficient and very fast gradient separations of peptides were realized [72]. A disadvantage of both silica- and polymer-monolithic materials is the heterogeneity of the macropore structure, affecting the magnitude of the *A*- and C_m-term contribution. Wouters *et al.* demonstrated that polymer monolithic columns with smaller characteristic size where characterized

by a relatively high *A*- and C_m-terms induced by structural inhomogeneity [73]. This implies that the conventional synthesis methods utilized to create short columns containing an interconnected structure of nanoglobules and submicron macropores may fall short with respect to heterogeneity. An alternative and promising synthesis approach is the γ-ray induced polymerization explored by the Gasparrini research group to synthesize polymethacylate monolithic capillary columns [74,75]. The morphology has been optimized towards kinetic performance and columns have been successfully applied yielding high-efficiency separations of both small molecules and peptides [74].

An alternative column format for high demanding separations are the open-tubular columns. Due to the very high column permeability of coated capillary columns this column type allows the use of very long column formats, albeit at the expense of a long analysis time [76]. To account for the low phase ratio, Causon *et al.* revisited the kinetic-plot approach taking into account kinetic performance in terms of time and efficiency, and also mass loadability [77]. It was demonstrated that to achieve good kinetic performance, relatively long coated capillary columns with very small I.D. (< 6 μm) need to be developed that are covered with a thick layer of porous material filling 50-70% of the column I.D. Forster *et al.* created 10-20 μm I.D. coated capillary columns covered with 230 up to 570 nm thick mesoporous silica [78]. Hara *et al.* adopted this strategy and developed up to 2.5 m long coated capillary of 5 μm in I.D. covered with mesoporous silica layers up to 550 nm yielding 1,000,000 plates for the unretained marker and up to 600,000 for retained analytes [79].

The current state-of-the-art high-throughput separations constitute sub-second separations reported by the Armstrong research group [80]. Patel *et al.* described ultra-fast separations of over 60 pairs of enantiomers within the 4-40 s range [81]. In a follow-up study, Wahab *et al.* demonstrated a sub-second HILIC separation of mellitic acid, 2,3-dihydroxybenzoic acid, and 4-aminosalicylic acid operating a 4.6 mm I.D. × 0.5 cm long column packed with 2.7 μm core-shell particles using an optimized UHPLC set-up with respect to extra column dispersion time delays [80]. To account for the asymmetric (tailing) peak shapes induced extra-column effects resulting in partial coelution of the

analytes, the raw data was subjected to a power transform yielding a baseline separation and gaussian peak profiles. In a recent study the Armstrong research group pushed the limits further and presented the sub-second separation of 10 analytes, see Fig. 9A for the raw data and Fig. 9B after Fourier transform deconvolution [82]. The sub-second separations were repeatable with 0.9% RSD on retention time. In gradient mode, Vaast described the separation of a mixture of 5 peptides on a 25 mm long monolithic bed applying 15 s ballistic gradients at 800 bar (total cycle time of 48 s) [83]. To realize separations with very high resolving power to accommodate for the sample complexity as can be encountered in life-science research and clinical diagnostics, long columns and column-coupling strategies [84-87] have been utilized in combination with the application of shallow gradients. For example, Grinias *et al.* designed a UHPLC system integrating gradient storage loops allowing to work in constant pressure mode up to 3100 bar and systematically investigated the chromatographic performance limits of capillary columns packed with fully-porous particles for the separation of protein digests [88]. Figure 9C shows how the run time is affected when smaller particles are used, while gradient steepness, operating pressure (2000 bar), and nominal flow rate (300 nL/min) are maintained [88].

6. Concluding remarks

To assess the chromatographic performance, different performance indices have been discussed that incorporate both separation efficiency and the pressure drop. To get the most expanded view on performance limits in terms of analysis time and efficiency, allowing for an unbiased comparison of chromatographic columns, kinetic plots can be constructed from experimental separation performance (as function of mobile-phase velocity) and pressure data. Expressions that quantify the gain in analysis time or efficiency in isocratic LC mode when enhancing the pressure limit of system (ΔP_{max}) or changing the characteristic feature size of chromatographic support structures (affecting H and/or $K_{v,0}$) have been reviewed. Furthermore, different visualization

approaches have been discussed. The 'Poppe plot', depicting the plate time (t_0/N) as function of plate number (N) provides an excellent representation mode to compare mass-transfer effects to chromatographic dispersion of different chromatographic supports. The t_0/N^2 *versus* N representation, provides a clear view on *B*-, and *C*-term contributions to band broadening and the minimum in the curve represents the minimum separation impedance (E_{min}) of a separation system.

UHPLC systems with a maximum pressure rating between 1300 up to 1500 bar have become readily available. Different system designs have been optimized towards maintaining the high separation efficiencies provided by 2.1 mm I.D. column formats packed with sub-2-micron stationary-phase particles. Furthermore, different solutions have been realized to addresses mobile-phase compression and mitigate axial and radial temperature gradients that may affect selectivity and separation efficiency. This could only be realized by completely redesigning parts of the UHPLC instrument and by utilizing new materials with a high mechanical stability. Also, the potential of extreme-pressure LC systems up to 7000 bar have already been demonstrated (with capillary column formats). The gold standard in separation science with respect to column technology remains the microparticulate columns. Compared to columns packed with fully-porous particles, core-shell particle-packed columns provide better kinetic performance limits due to reduce *A*-, *B*-, and *C*-term contributions and the higher column permeability. High-peak capacity separations have been realized using long (up to 1 m) columns and coupled-column system working close to the maximum system pressure. Finally, a break-through in performance limits has been presented by the Armstrong research group, who have demonstrated sub-second separations of a wide range of enantiomers, and for separations conducted in HILIC mode.

7. Acknowledgements

JLDS, JDV, and SE acknowledge the Research Foundation Flanders (FWO) for financial support (grant no. G025916N, 12J6517N, and 1508914N, respectively).

8. References

[1] Ettre, L. S., M.S. Tswett and the invention of chromatography. *LC GC North Am* 2003, *21*, 458-467.

[2] Ettre, L. S., Key moments in the evolution of liquid chromatography. *J. Chromatogr.* 1990, *535*, 3-12.

[3] Robards, K., Haddad, P. R., Jackson, P. E., in: Robards, K., Haddad, P. R., Jackson, P. E. (Eds.), Principles and Practice of Modern Chromatographic Methods, Academic Press, Boston 2004, pp. 1-34.

[4] Orna, M. V., The Chemical History of Color, Springer, Heidelberg 2013.

[5] Martin, A. J. P., Synge, R. L. M., A new form of chromatogram employing two liquid phases. *Biochem. J*. 1941, *35*, 1358-1368.

[6] Horvath, C. G., Preiss, B. A., Lipsky, S. R., Fast liquid chromatography: an investigation of operating parameters and the separation of nucleotides on pellicular ion exchangers. *Anal. Chem.* 1967, *39*, 1422-1428.

[7] Snyder, L. R., HPLC: past and present. *Anal. Chem.* 2000, *72*, 412a-420a.

[8] Neue, U. D., HPLC Columns: Theory, Technology, and Practice, Wiley-VCH, New York 1997.

[9] Gritti, F., Guiochon, G., The current revolution in column technology: How it began, where is it going?, *J. Chromato gr. A* 2012, *1228*, 2-19.

[10] Neue, U. D., Serowik, E., Iraneta, P., Alden, B. A., Walter, T. H., Universal procedure for the assessment of the reproducibility and the classification of silica-based reversed-phase packings: I. Assessment of the reproducibility of reversed-phase packings. *J. Chromatogr. A* 1999, *849*, 87-100.

[11] MacNair, J. E., Lewis, K. C., Jorgenson, J. W., Ultrahigh-pressure reversed-phase liquid chromatography in packed capillary columns. *Anal. Chem.* 1997, *69*, 983-989.

[12] Mazzeo, J. R., D.Neue, U., Kele, M., Plumb, R. S., Advancing LC Performance with Smaller Particles and Higher Pressure. *Anal. Chem.* 2005, *77*, 460 A-467 A.

[13] Blue, L. E., Franklin, E. G., Godinho, J. M., Grinias, J. P., Grinias, K. M., Lunn, D. B., Moore, S. M., Recent advances in capillary ultrahigh pressure liquid chromatography. *J. Chromatogr. A* 2017, *1523*, 17-39.

[14] Walter, T. H., Andrews, R. W., Recent innovations in UHPLC columns and instrumentation. *TrAC-Trends Anal. Chem.* 2014, *63*, 14-20.

[15] Giddings, J. C., Unified Separation Science, Wiley-Interscience, New York 1991.

[16] Purnell, J. H., 256. The correlation of separating power and efficiency of gas-chromatographic columns. *J. Chem. Soc.* 1960, 1268-1274.

[17] Foley, J. P., Resolution equations for column chromatography. *Analyst* 1991, *116*, 1275-1279.

[18] Sandra, P., Resolution–definition and nomenclature. *J. High Resol. Chromatogr.* 1989, *12*, 82-86.

[19] Eeltink, S., Decrop, W. M., Steiner, F., Ursem, M., Cabooter, D., Desmet, G., Kok, W. T., Use of kinetic plots for the optimization of the separation time in ultra-high-pressure LC. *J. Sep. Sci.* 2010, *33*, 2629-2635.

[20] Giddings, J. C., Dynamics of Chromatography: Principles and Theory, Marcel Dekker Inc, New York 1965.

[21] van Deemter, J. J., Zuiderweg, F. J., Klinkenberg, A., Longitudinal diffusion and resistance to mass transfer as causes of nonideality in chromatography. *Chem. Engng. Sci.* 1956, *5*, 271-289.

[22] Gritti, F., Guiochon, G., Mass transfer kinetics, band broadening and column efficiency. *J. Chromatogr. A* 2012, *1221*, 2-40.

[23] Knox, J. H., Practical Aspects of LC Theory. *J. Chromatogr. Sci.* 1977, *15*, 352-364.

[24] Bristow, P. A., Knox, J. H., Standardization of test conditions for high performance liquid chromatography columns. *Chromatographia* 1977, *10*, 279-289.

[25] Giddings, J. C., Comparison of theoretical limit of separating speed in gas and liquid chromatography. *Anal. Chem.* 1965, *37*, 60-63.

[26] Desmet, G., Clicq, D., Gzil, P., Geometry-independent plate height representation methods for the direct comparison of the kinetic performance of LC supports with a different size or morphology. *Anal. Chem.* 2005, *77*, 4058-4070.

[27] Andrés, A., Broeckhoven, K., Desmet, G., Methods for the experimental characterization and analysis of the efficiency and speed of chromatographic columns: A step-by-step tutorial. *Anal. Chim. Acta* 2015, *894*, 20-34.

[28] Cabooter, D., Lestremau, F., Lynen, F., Sandra, P., Desmet, G., Kinetic plot method as a tool to design coupled column systems producing 100,000 theoretical plates in the shortest possible time. *J. Chromatogr. A* 2008, *1212*, 23-34.

[29] Cabooter, D., Lestremau, F., de Villiers, A., Broeckhoven, K., Lynen, F., Sandra, P., Desmet, G., Investigation of the validity of the kinetic plot method to predict the performance of coupled column systems operated at very high pressures under different thermal conditions. *J. Chromatogr. A* 2009, *1216*, 3895-3903.

[30] de Villiers, A., Lestremau, F., Szucs, R., Gélébart, S., David, F., Sandra, P., Evaluation of ultra performance liquid chromatography: Part I. Possibilities and limitations. *J. Chromatogr. A* 2006, *1127*, 60-69.

[31] De Vos, J., De Pra, M., Desmet, G., Swart, R., Edge, T., Steiner, F., Eeltink, S., High-speed isocratic and gradient liquid-chromatography separations at 1500 bar. *J. Chromatogr. A* 2015, *1409*, 138-145.

[32] De Vos, J., Broeckhoven, K., Eeltink, S., Advances in ultrahigh-pressure liquid chromatography technology and system design. *Anal. Chem.* 2016, *88*, 262-278.

[33] Knox, J. H., Saleem, M., Kinetic conditions for optimum speed and resolution in column chromatography. *J. Chromatogr. Sci.* 1969, *7*, 614-622.

[34] Broeckhoven, K., Desmet, G., The future of UHPLC: Towards higher pressure and/or smaller particles? *TrAC-Trends Anal. Chem.* 2014, *63*, 65-75.

[35] Blumberg, L. M., Desmet, G., Kinetic performance factor – A measurable metric of separation-time-pressure tradeoff in liquid and gas chromatography, *J. Chromatogr. A* 2018, 1567, 26-36.

[36] Eeltink, S., Gzil, P., Kok, W. T., Schoenmakers, P. J., Desmet, G., Selection of comparison criteria and experimental conditions to evaluate the kinetic performance of monolithic and packed-bed columns. *J. Chromatogr. A* 2006, *1130*, 108-114.

[37] Neue, U. D., Theory of peak capacity in gradient elution. *J. Chromatogr. A* 2005, *1079*, 153-161.

[38] Dolan, J. W., Snyder, L. R., Djordjevic, N. M., Hill, D. W., Waeghe, T. J., Reversed-phase liquid chromatographic separation of complex samples by optimizing temperature and gradient time: I. Peak capacity limitations. *J. Chromatogr. A* 1999, *857*, 1-20.

[39] Broeckhoven, K., Cabooter, D., Lynen, F., Sandra, P., Desmet, G., The kinetic plot method applied to gradient chromatography: Theoretical framework and experimental validation. *J. Chromatogr. A* 2010, *1217*, 2787-2795.

[40] Causon, T. J., Broeckhoven, K., Hilder, E. F., Shellie, R. A., Desmet, G., Eeltink, S., Kinetic performance optimisation for liquid chromatography: Principles and practice. *J. Sep. Sci.* 2011, *34*, 877-887.

[41] Ruegenberg, G., Schloderer, R., Tuchan, W., Control arrangements for controlling a piston pump unit for liquid chromatography. U.S. Patent Application 20130336803 A1, December 19, 2013.

[42] Steiner, F., in: Kromidas, S. (Ed.), The HPLC Expert II, Wiley-VCH, Weinheim, 2017.

[43] de Villiers, A., Lauer, H., Szucs, R., Goodall, S., Sandra, P., Influence of frictional heating on temperature gradients in ultra-high-pressure liquid chromatography on 2.1 mm I.D. columns. *J. Chromatogr. A* 2006, *1113*, 84-91.

[44] Gritti, F., Guiochon, G., Measurement of the axial and radial temperature profiles of a chromatographic column. Influence of thermal insulation on column efficiency. *J. Chromatogr. A* 2007, *1138*, 141-157.

[45] Patel, K. D., Jerkovich, A. D., Link, J. C., Jorgenson, J. W., In-depth characterization of slurry packed capillary columns with 1.0-μm nonporous particles using reversed-phase isocratic ultrahigh-pressure liquid chromatography. *Anal. Chem.* 2004, *76*, 5777-5786.

[46] Vanderheyden, Y., Cabooter, D., Desmet, G., Broeckhoven, K., Isocratic and gradient impedance plot analysis and comparison of some recently introduced large size core–shell and fully porous particles. *J. Chromatogr. A* 2013, *1312*, 80-86.

[47] Reising, A. E., Godinho, J. M., Bernzen, J., Jorgenson, J. W., Tallarek, U., Axial heterogeneities in capillary ultrahigh pressure liquid chromatography columns: Chromatographic and bed morphological characterization. *J. Chromatogr. A* 2018, *in press*.

[48] Reising, A. E., Godinho, J. M., Hormann, K., Jorgenson, J. W., Tallarek, U., Larger voids in mechanically stable, loose packings of 1.3 μm frictional, cohesive particles: Their reconstruction, statistical analysis, and impact on separation efficiency. *J. Chromatogr. A* 2016, *1436*, 118-132.

[49] Billen, J., Guillarme, D., Rudaz, S., Veuthey, J.-L., Ritchie, H., Grady, B., Desmet, G., Relation between the particle size distribution and the kinetic performance of packed columns. Application to a commercial sub-2 μm particle material. *J. Chromatogr. A* 2007, *1161*, 224-233.

[50] Bruns, S., Stoeckel, D., Smarsly, B. M., Tallarek, U., Influence of particle properties on the wall region in packed capillaries. *J. Chromatogr. A* 2012, *1268*, 53-63.

[51] DeStefano, J. J., Schuster, S. A., Lawhorn, J. M., Kirkland, J. J., Performance characteristics of new superficially porous particles. *J. Chromatogr. A* 2012, *1258*, 76-83.

[52] Tanaka, N., McCalley, D. V., Core–shell, ultrasmall particles, monoliths, and other support materials in high-performance liquid chromatography. *Anal. Chem.* 2016, *88*, 279-298.

[53] Broeckhoven, K., Cabooter, D., Desmet, G., Kinetic performance comparison of fully and superficially porous particles with sizes ranging between 2.7 μm and 5 μm: Intrinsic evaluation and application to a pharmaceutical test compound. *J. Pharm. Anal.* 2013, *3*, 313-323.

[54] Wei, T.-C., Mack, A., Chen, W., Liu, J., Dittmann, M., Wang, X., Barber, W. E., Synthesis, characterization, and evaluation of a superficially porous particle with unique, elongated pore channels normal to the surface. *J. Chromatogr. A* 2016, *1440*, 55-65.

[55] Deridder, S., Catani, M., Cavazzini, A., Desmet, G., A theoretical study on the advantage of core-shell particles with radially-oriented mesopores. *J. Chromatogr. A* 2016, *1456*, 137-144.

[56] Svec, F., Monolithic columns: A historical overview. *Electrophoresis* 2017, *38*, 2810-2820.

[57] Ikegami, T., Tanaka, N., Recent progress in monolithic silica columns for high-speed and high-selectivity separations. *Annu. Rev. Anal. Chem. (Palo Alto Calif)* 2016, *9*, 317-342.

[58] Liu, K., Aggarwal, P., Lawson, J. S., Tolley, H. D., Lee, M. L., Organic monoliths for high-performance reversed-phase liquid chromatography. *J. Sep. Sci.* 2013, *36*, 2767-2781.

[59] Eeltink, S., Wouters, S., Dores-Sousa, J. L., Svec, F., Advances in organic polymer-based monolithic column technology for high-resolution liquid chromatography-mass spectrometry profiling of antibodies, intact proteins, oligonucleotides, and peptides. *J. Chromatogr. A* 2017, *1498*, 8-21.

[60] Guiochon, G., Monolithic columns in high-performance liquid chromatography. *J. Chromatogr. A* 2007, *1168*, 101-168.

[61] Motokawa, M., Kobayashi, H., Ishizuka, N., Minakuchi, H., Nakanishi, K., Jinnai, H., Hosoya, K., Ikegami, T., Tanaka, N., Monolithic silica columns with various skeleton sizes and through-pore sizes for capillary liquid chromatography. *J. Chromatogr. A* 2002, *961*, 53-63.

[62] Horie, K., Kamakura, T., Ikegami, T., Wakabayashi, M., Kato, T., Tanaka, N., Ishihama, Y., Hydrophilic interaction chromatography using a meter-scale monolithic silica capillary column for proteomics LC-MS. *Anal. Chem.* 2014, *86*, 3817-3824.

[63] Cabrera, K., Lubda, D., Eggenweiler, H.-M., Minakuchi, H., Nakanishi, K., A new monolithic-type HPLC column for fast separations. *J. High Resol. Chromatogr.* 2000, *23*, 93-99.

[64] Tanaka, N., Nagayama, H., Kobayashi, H., Ikegami, T., Hosoya, K., Ishizuka, N., Minakuchi, H., Nakanishi, K., Cabrera, K., Lubda, D., Monolithic Silica Columns for HPLC, Micro-HPLC, and CEC. *J. High Resol. Chromatogr.* 2000, *23*, 111-116.

[65] Ishizuka, N., Kobayashi, H., Minakuchi, H., Nakanishi, K., Hirao, K., Hosoya, K., Ikegami, T., Tanaka, N., Monolithic silica columns for high-efficiency separations by high-performance liquid chromatography. *J. Chromatogr. A* 2002, *960*, 85-96.

[66] Vuignier, K., Fekete, S., Carrupt, P. A., Veuthey, J. L., Guillarme, D., Comparison of various silica-based monoliths for the analysis of large biomolecules. *J. Sep. Sci.* 2013, *36*, 2231-2243.

[67] Xie, C., Ye, M., Jiang, X., Jin, W., Zou, H., Octadecylated silica monolith capillary column with integrated nanoelectrospray ionization emitter for highly efficient proteome analysis. *Mol. Cell. Proteomics* 2006, *5*, 454-461.

[68] Horie, K., Sato, Y., Kimura, T., Nakamura, T., Ishihama, Y., Oda, Y., Ikegami, T., Tanaka, N., Estimation and optimization of the peak capacity of one-dimensional gradient high performance liquid chromatography using a long monolithic silica capillary column. *J. Chromatogr. A* 2012, *1228*, 283-291.

[69] Courtois, J., Byström, E., Irgum, K., Novel monolithic materials using poly(ethylene glycol) as porogen for protein separation. *Polymer* 2006, *47*, 2603-2611.

[70] Viklund, C., Nordström, A., Irgum, K., Svec, F., Fréchet, J. M. J., Preparation of porous poly(styrene-*co*-divinylbenzene) monoliths with controlled pore size distributions initiated by stable free radicals and their pore surface functionalization by grafting. *Macromolecules* 2001, *34*, 4361-4369.

[71] Viklund, C., Svec, F., Fréchet, J. M. J., Irgum, K., Monolithic, "molded", porous materials with high flow characteristics for separations, catalysis, or solid-phase chemistry: control of porous properties during polymerization. *Chem. Mater.* 1996, *8*, 744-750.

[72] Vaast, A., Terryn, H., Svec, F., Eeltink, S., Nanostructured porous polymer monolithic columns for capillary liquid chromatography of peptides. *J. Chromatogr. A* 2014, *1374*, 171-179.

[73] Wouters, S., Hauffman, T., Mittelmeijer-Hazeleger, M. C., Rothenberg, G., Desmet, G., Baron, G. V., Eeltink, S., Comprehensive study of the macropore and mesopore size distributions in polymer monoliths using complementary physical characterization techniques and liquid chromatography. *J. Sep. Sci.* 2016, *39*, 4492-4501.

[74] Simone, P., Pierri, G., Capitani, D., Ciogli, A., Angelini, G., Ursini, O., Gentile, G., Cavazzini, A., Villani, C., Gasparrini, F., Capillary methacrylate-based monoliths by grafting from/to γ-ray polymerization on a tentacle-type reactive surface for the liquid chromatographic separations of small molecules and intact proteins. *J. Chromatogr. A* 2017, *1498*, 46-55.

[75] Simone, P., Pierri, G., Foglia, P., Gasparrini, F., Mazzoccanti, G., Capriotti, A. L., Ursini, O., Ciogli, A., Laganà, A., Separation of intact proteins on γ-ray-induced polymethacrylate monolithic columns: A highly permeable stationary phase with high peak capacity for capillary high-performance liquid chromatography with high-resolution mass spectrometry. *J. Sep. Sci.* 2016, *39*, 264-271.

[76] Kucera, P., Guiochon, G., Use of open-tubular columns in liquid chromatography. *J. Chromatogr. A* 1984, *283*, 1-20.

[77] Causon, T. J., Shellie, R. A., Hilder, E. F., Desmet, G., Eeltink, S., Kinetic optimisation of open-tubular liquid-chromatography capillaries coated with thick porous layers for increased loadability. *J. Chromatogr. A* 2011, *1218*, 8388-8393.

[78] Forster, S., Kolmar, H., Altmaier, S., Preparation and kinetic performance assessment of thick film 10-20 μm open tubular silica capillaries in normal phase high pressure liquid chromatography. *J. Chromatogr. A* 2013, *1315*, 127-134.

[79] Hara, T., Futagami, S., Eeltink, S., De Malsche, W., Baron, G. V., Desmet, G., Very high efficiency porous silica layer open-tubular capillary columns produced via in-column sol-gel processing. *Anal. Chem.* 2016, *88*, 10158–10166 .

[80] Wahab, M. F., Wimalasinghe, R. M., Wang, Y., Barhate, C. L., Patel, D. C., Armstrong, D. W., Salient sub-second separations. *Anal. Chem.* 2016, *88*, 8821-8826.

[81] Patel, D. C., Breitbach, Z. S., Wahab, M. F., Barhate, C. L., Armstrong, D. W., Gone in seconds: Praxis, performance, and peculiarities of ultrafast chiral liquid chromatography with superficially porous particles. *Anal. Chem.* 2015, *87*, 9137-9148.

[82] Patel, D. C., Wahab, M. F., O'Haver, T.C., Armstrong, D. W., Separations at the speed of sensors. *Anal. Chem.* 2018, *90*, 3349-3356.

[83] Vaast, A., Ultra-fast Capillary Gradient Liquid Chromatography of Biomolecules, PhD Thesis, Vrije Universiteit Brussel, Brussels, Belgium, 2014.

[84] Shen, Y., Zhang, R., Moore, R. J., Kim, J., Metz, T. O., Hixson, K. K., Zhao, R., Livesay, E. A., Udseth, H. R., Smith, R. D., Automated 20 kpsi RPLC-MS and MS/MS with chromatographic peak capacities of 1000-1500 and capabilities in proteomics and metabolomics. *Anal. Chem.* 2005, *77*, 3090-3100.

[85] Shen, Y., Tolic, N., Piehowski, P. D., Shukla, A. K., Kim, S., Zhao, R., Qu, Y., Robinson, E., Smith, R. D., Paša-Tolićb, L., High-resolution ultrahigh-pressure long column reversed-phase liquid chromatography for top-down proteomics. *J. Chromatogr. A* 2017, *1498*, 99-110.

[86] DeStefano, J. J., Boyes, B. E., Schuster, S. A., Miles, W. L., Kirkland, J. J., Are sub-2 μm particles best for separating small molecules? An alternative. *J. Chromatogr. A* 2014, *1368*, 163-172.

[87] De Vos, J., Stassen, C., Vaast, A., Desmet, G., Eeltink, S., High-resolution separations of tryptic digest mixtures using core-shell particulate columns operated at 1200 bar. *J. Chromatogr. A* 2012, *1264*, 57-62.

[88] Grinias, K. M., Godinho, J. M., Franklin, E. G., Stobaugh, J. T., Jorgenson, J. W., Development of a 45 kpsi ultrahigh pressure liquid chromatography instrument for gradient separations of peptides using long microcapillary columns and sub-2 μm particles. *J. Chromatogr. A* 2016, *1469*, 60-67.

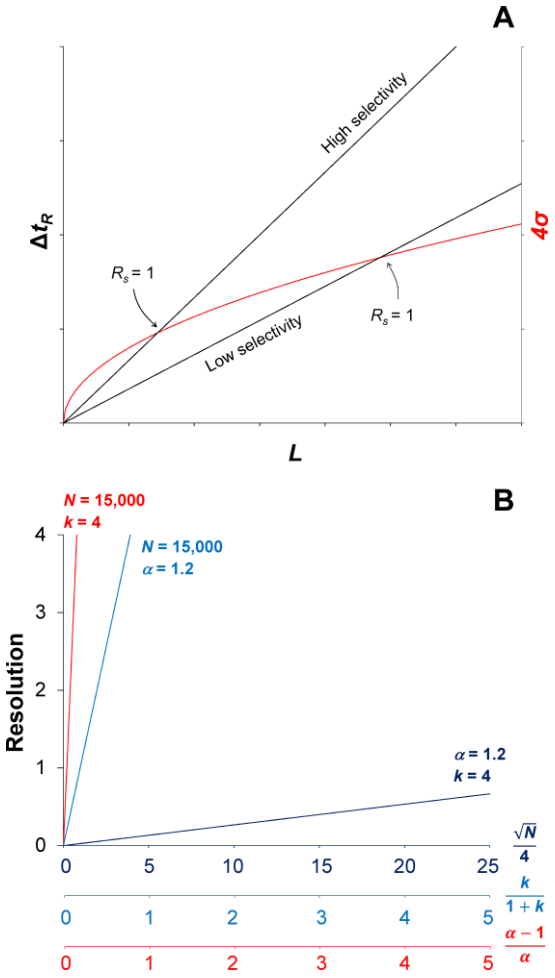

Figure 1. (A) Distance between two peaks centers (Δt_R) and peak width (4σ) as function of traveling distance (L) in chromatographic supports presenting low and high selectivity. With increasing selectivity Δt_R increases more rapidly with L, crossing the 4σ line sooner, generating unit resolution in a shorter migration distance. (B) Influence of efficiency (N), retention factor (k), and selectivity (α) on the resolution.

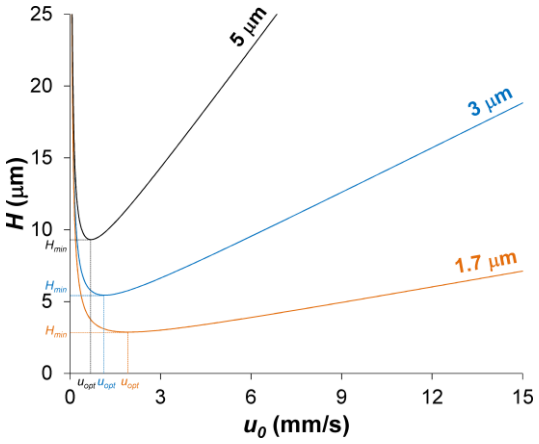

Figure 2. Van Deemter curves for columns packed with 5, 3, and 1.7 µm particles. The total plate heights (*H*) is the sum eddy dispersion (*A*-term), longitudinal diffusion (*B*-term), and resistance to mass transfer (*C*-term) contributions as function of mobile-phase velocity (u_0).

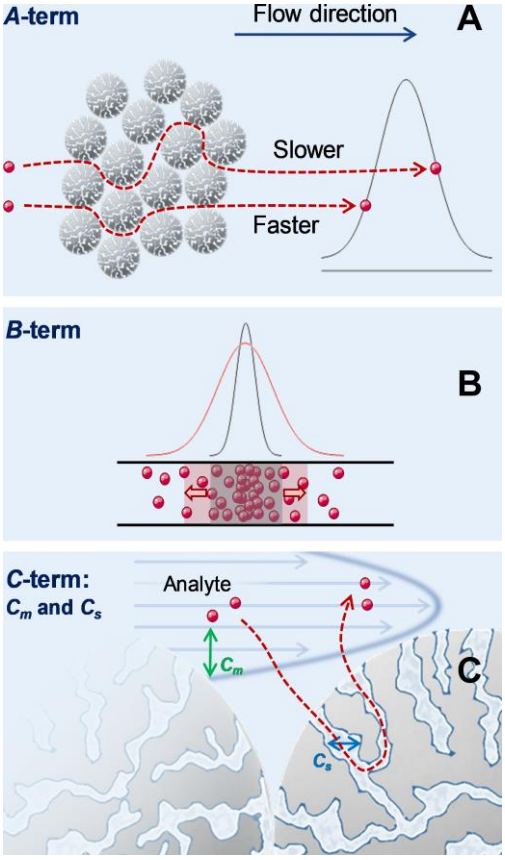

Figure 3. Schematic representation of the eddy dispersion (*A*-term), longitudinal diffusion (*B*-term), and resistance to mass-transfer (*C*-term) contributions to chromatographic dispersion.

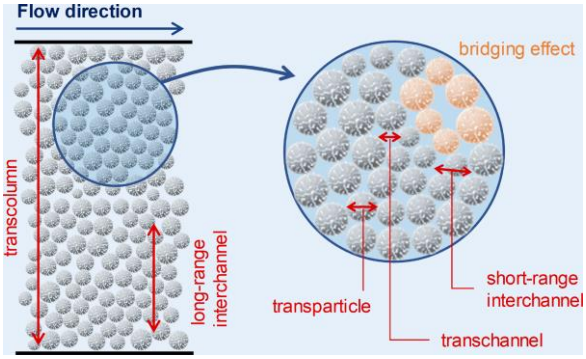

Figure 4. The location and distance covered by various exchange processes between velocity extremes in the mobile phase [20].

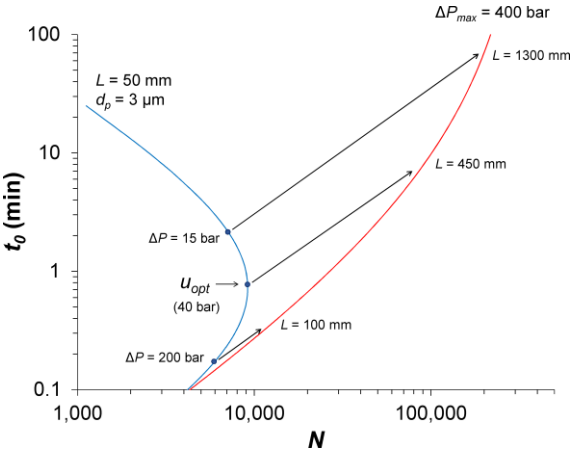

Figure 5. Construction of a kinetic plot from experimental van Deemter and pressure data to construct the performance limit curve when operating columns packed with 3 µm particles at a maximum operating pressure (ΔP_{max}) of 400 bar.

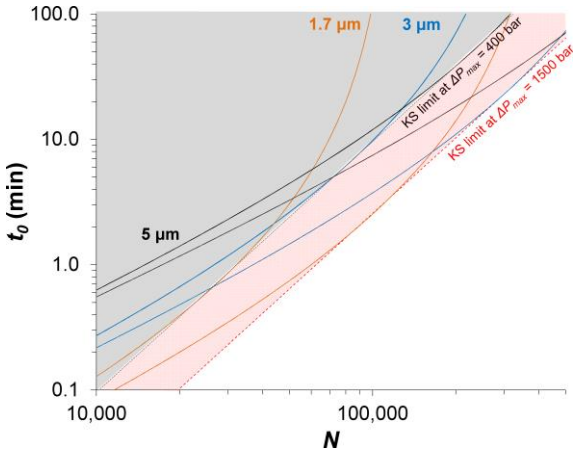

Figure 6. Performance limits curve of columns packed with 5, 3, and 1.7 µm particles operated at conventional HPLC conditions (400 bar in grade shade) *versus* UHPLC conditions (1500 bar in red shade).

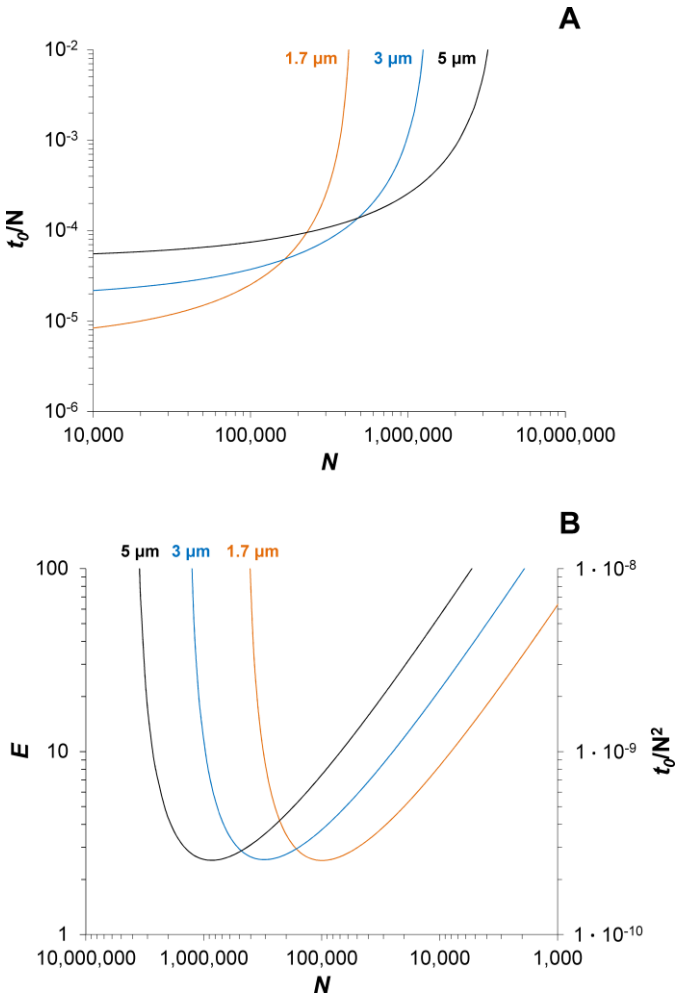

Figure 7. Different representations of kinetic plots: the 'Poppe plot' showing plate time *versus* plate number with (B) and the separation impedance as function of plate number (B). Performance limits are calculated for columns packed with 5, 3, and 1.7 µm particles applying a maximum operating pressure of 1500 bar.

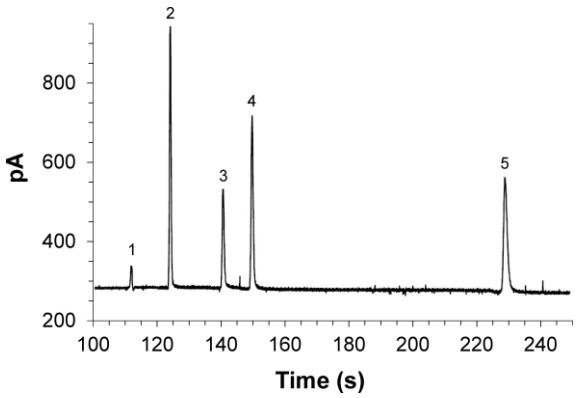

Figure 8. Chromatogram of an RP-LC separation of ascorbic acid (1) hydroquinone (2), resorcinol (3), catechol (4) obtained on a 10 μm I.D. × 43 cm column packed with 1 μm non-porous particles operated at 7100 bar yielding up to 310,000 plates. Adapted from [45] with permission.

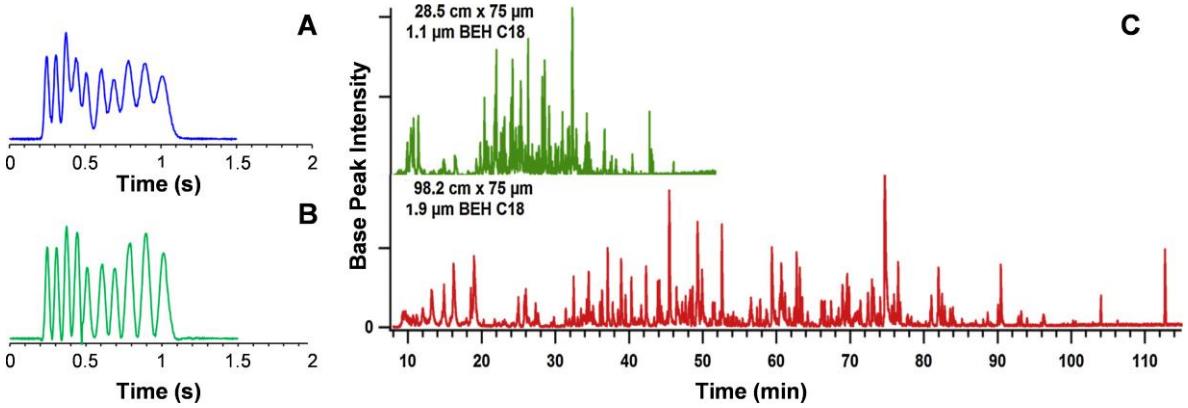

Figure 9. State-of-the-art high separations demonstrating the current performance limits in liquid chromatography: a sub-second HILIC separation of a mixture of 10 analytes obtained on a 0.3 cm I.D. × 1 cm long column packed with 1.9 μm core-shell particles operated at 8 mL/min; (A) depicts the raw data and (B) show the data after applying peak deconvolution and a segmented derivative peak sharpening enhancement (adapted from [82] with permission). (C) shows high peak capacity gradient separation of tryptic peptides and demonstrates how run time is affected applying columns packed with fully-porous particles with while maintaining the gradient steepness, operating pressure, and nominal flow rate constant (adapted from [88] with permission).